Frontiers in Flow Cytometry™

A 24 hour Virtual Event by Thermo Fisher Scientific

Want to discover the latest advances in strategies & applications in flow cytometry?

Frontiers in Flow Cytometry is aimed at researchers across the globe looking for an opportunity to share current developments in flow cytometry.
Key topics include:

- Spectral and conventional flow cytometry
- Immunophenotyping
- Panel design and optimization
- Infectious diseases
- Advances in flow cytometry technology

This 24 hour virtual event will feature keynote presentations and industry colleagues, webinars, demos, live networking opportunities and more.

Join the conversation with your colleagues around the world. We are kicking off the event on May 17 at 8am SGT; 2am CEST; and 5pm PDT (May 16th).
#FrontiersInFlow

REGISTER NOW

Flow Cytometry-Based High-Throughput RNAi Screening for miRNAs Regulating MHC Class II HLA-DR Surface Expression

Journal:	*European Journal of Immunology - 2*
Manuscript ID	eji.202149735.R2
Wiley - Manuscript type:	Research Article
Date Submitted by the Author:	17-May-2022
Complete List of Authors:	Houseman, Maja; Inselspital Universitatsspital Bern, Universitätsklinik für Anästhesiologie und Schmerztherapie Huang, Melody Ying-Yu; Inselspital Universitatsspital Bern, Universitätsklinik für Anästhesiologie und Schmerztherapie; ETH-Bereich Hochschulen, HEST Huber, Markus ; Inselspital Universitatsspital Bern, Universitätsklinik für Anästhesiologie und Schmerztherapie Staiger, Matthias ; Inselspital Universitatsspital Bern, Universitätsklinik für Anästhesiologie und Schmerztherapie Zhang, Lan ; Inselspital Universitatsspital Bern, Universitätsklinik für Anästhesiologie und Schmerztherapie Hoffmann, Anneliese ; Inselspital Universitatsspital Bern, Universitätsklinik für Anästhesiologie und Schmerztherapie Lippuner, Christoph ; Inselspital Universitatsspital Bern, Universitätsklinik für Anästhesiologie und Schmerztherapie Stüber, Frank ; Inselspital Universitatsspital Bern, Universitätsklinik für Anästhesiologie und Schmerztherapie
Keywords:	human leukocyte antigen (HLA), antigen-presenting cells (APCs), MHC class II, microRNA (miRNA), transfection
Keywords:	
Note: The following files were submitted by the author for peer review, but cannot be converted to PDF. You must view these files (e.g. movies) online.	
Graphical abstract_image.tif	

Flow Cytometry-Based High-Throughput RNAi Screening for miRNAs Regulating MHC Class II HLA-DR Surface Expression

Maja Houseman[1,2,*], Melody Ying-Yu Huang[1,2,3,*,✉], Markus Huber[1,2], Matthias Staiger[1,2], Lan Zhang[1,2], Anneliese Hoffmann[1,2], Christoph Lippuner[1,2] and Frank Stüber[1,2,✉]

[1]Department of Anaesthesiology and Pain Medicine, Inselspital, Bern University Hospital, University of Bern, Bern, Switzerland

[2]Department for BioMedical Research, University of Bern, Bern, Switzerland

[3]Department of Health Sciences and Technology, Swiss Federal Institute of Technology (ETH) Zürich, Zürich, Switzerland

*Co-first authorship

✉Corresponding authors:

Melody Ying-Yu Huang, Universitätsklinik für Anästhesiologie und Schmerztherapie, Inselspital, 3010, Bern; melody.yingyu.huang@gmail.com

Frank Stüber, Universitätsklinik für Anästhesiologie und Schmerztherapie, Inselspital, 3010, Bern; frank.stueber@insel.ch

Short running title: HLA-DR regulation by miRNAs

Keywords: MHC class II; human leukocyte antigen (HLA); antigen-presenting cells (APCs); microRNA (miRNA); transfection

List of abbreviations used 3 or more times in the text

APCs	antigen-presenting cells
HLA	human leukocyte antigen
miRNA	microRNA
RNAi	ribonucleic acid interference
MHC	major histocompatibility class

FCM	flow cytometry
qPCR	quantitative real-time PCR

Abstract

Human leukocyte antigen–DR isotype (HLA-DR) is a major histocompatibility class II (MHC-II) cell surface receptor found on antigen-presenting cells (APCs) and plays a key role in initiating immune responses. In severely immunocompromised patients with conditions like sepsis, the number of HLA-DR molecules expressed on leukocytes is considered to correlate with infectious complications and patients' probability of survival. The underlying regulatory mechanisms of HLA-DR expression remain largely unknown. One probable path to regulation is through microRNAs (miRNAs), which have been implicated as regulatory elements of both innate and adaptive immune system development and function. In our study, flow cytometry-based high-throughput miRNA screening was performed in a stable HLA-DR-expressing human melanoma cell line, MelJuSo, for either up- or down-regulating miRNAs of the surface HLA-DR expression. By the end of the screening, the top ten up-regulators and top five down-regulators were identified, and both the HLA-DR protein and mRNA regulations were further verified and validated. In silico approaches were applied for functional miRNA-mRNA interaction prediction. The potential underlying gene regulations of different miRNAs were proposed. Our results promote the study of miRNA-mediated HLA-DR regulation under both physiological and pathological conditions, and may pave the way for potential clinical applications.

Introduction

Major histocompatibility complex class I/II molecules (MHC-I/II) are important proteins that play a critical role in the immune response. Human leukocyte antigen–DR isotype (HLA-DR) is an MHC-II cell surface receptor typically found on professional antigen-presenting cells (APCs), such as monocytes or dendritic cells. The primary function of HLA-DR is to display processed antigens on APCs to appropriate immune cells, such as cluster of differentiation 4 (CD4)+ T-cells;[1] however, activation of HLA-DR expression in CD8+ cytotoxic T-cells has also been associated with autoimmune diseases, HIV, and breast cancer.[2-4] Clinically, decreased HLA-DR surface expression levels on CD14+ monocytes have been shown to correlate with higher mortality in sepsis, or to demonstrate a higher risk of acquiring severe nosocomial infections.[5]

Besides decreased HLA-DR surface expression, the other frequently used clinical indicator of monocytic immune incapacity associated with immunosuppression is decreased levels of *ex vivo* lipopolysaccharide-induced tumor necrosis factor alpha production. However, with the latter not being able to reliably distinguish among disease severity levels, monocytic HLA-DR surface expression may prove to be a more accurate predictor of mortality and/or acquisition of nosocomial infections in critically ill patients from surgical or medical intensive care units.[6-11] Recently, monocytic HLA-DR surface expression was used as one critical immunological parameter in monitoring severe cases of coronavirus disease 2019 (COVID-19).[12-15]

During biological processes, protein expression can be regulated by several mechanisms, one of which is ribonucleic acid (RNA) interference (RNAi), the interaction of small interference RNA (siRNA) or micro RNA (miRNA) with messenger RNA (mRNA). A high-throughput RNAi screening detecting HLA-DR surface expression may pave the way for development of new therapeutic approaches and for identifying novel peripheral blood biomarkers of severe infections.

In a previous study, a systematic genome-wide flow cytometry (FCM)-based siRNA screening targeting MHC-II expression and peptide loading revealed factors and underlying transcriptional networks and transport pathways of MHC-II regulation that may be linked to infection and autoimmunity.[16] For instance, TGFβ signaling may be involved in MHC-II transcriptional regulation via RMND5B and SMADs. Further, a pathway of the GTPase ARL14/ARF7 and actin-based motor myosin 1E has been linked to the MHC-II transport controls in dendritic cells. In contrast to siRNA, little has

been reported with regard to miRNA's involvement in MHC-II regulation. siRNA and miRNA, which differ mainly in their mRNA target-binding specificity, possess mechanisms of action and clinical applications which are not yet distinct.

In the current study, we used a stable MHC-II-expressing human melanoma cell line, MelJuSo,[16,17] to perform FCM-based high-throughput miRNA screening for the first time. The aim was to identify miRNAs with either up- or down-regulating activity of surface HLA-DR expression. To ensure the suitability and high quality of our screening assay, we computed the screening window coefficient Z'-factor for the assay quality assessment.[18] Moreover, we applied a statistical method that is intended specifically for cell-based RNAi screening analysis, which takes into account the considerable between-plate variation found in the cytometry methods.[19]

According to the calculated rank order, we identified ten HLA-DR up-regulating and five down-regulating miRNA candidates from ~2000 human miRNA compounds stored in the miRIDIAN miRNA mimic library. By the end of the RNAi screening, we had successfully verified the miRNA regulation of surface HLA-DR expression with separate FCM assays. Furthermore, we validated the RNAi effect on the *HLA-DRA* mRNA expression using quantitative real-time PCR (*qPCR*) and compared the results with those of the protein regulation.

Results

Large-scale miRNA screen

Instead of using antigen-presenting cells (APCs), we chose the human melanoma cell line MelJuSo, which has stable constitutive HLA-DR surface expression but lacks many other immune-specific gene expressions. This was used to perform a large-scale, high-throughput flow cytometry (FCM)-based screening for miRNA candidates regulating the HLA-DR surface expression. With this approach we were better able to focus on the miRNA-regulated HLA-DR pathways by avoiding certain indirect RNAi-modulated HLA-DR expression alterations via other immune factors. Toll-like receptors (TLRs), for example, are known to interact with antisense and siRNA.[16,20,21]

A total of ~2000 miRNA mimics from the miRIDIAN miRNA mimic library (see Methods) were individually transfected into MelJuSo cells on 96-well plates. The siRNA Hs_CIITA_2, targeting the MHC-II transactivator CIITA, known to down-regulate CIITA and thus HLA-DR, was employed in our transfection assay as the positive control.[22,23] In addition, two *C. elegans* miRNAs–cel-miR-67 and cel-miR-239b–which have no known target sequence in human cells, were included as negative controls.

To visualize the regulatory effect of miRNA on HLA-DR surface expression in MelJuSo cells, a monoclonal mouse anti-human HLA-DR antibody detecting peptide-loaded MHC-II/HLA-DR was used for cell surface staining prior to the FCM analysis.[24] All experiments were performed three times. The overall cell viability of our transfection assay was estimated to be 88%, which was calculated using the fixable viability dye eFluor™ 506 (eBioscience). Moreover, the miRNA transfection efficiency in MelJuSo cells was estimated to be more than 90% according to the Dy547-labelled miRNA hairpin inhibitor transfection control.

First, we applied the FCM analysis and computed the median fluorescent intensity (MFI) of each individual well. Next, to ensure and validate the quality of the RNAi assays, we adapted a statistical method and computed the *Z'*-factor, a popular parameter for HTS experiments (see Methods).[18,19] Figure 1 shows box plots of MFIs of the three experimental sets of the FCM data, grouped by plate A and B (A1-A25, B1-B25) and sample type (sample, positive and negative controls). In both A and B experiments, the assignment of miRNAs to plates was quasi randomized; however, as shown in Figures 1A and 1B, the absolute MFI values varied across plates. In addition, a similar plate-specific MFI pattern was observed among samples (Fig. 1A-B) and

controls (Fig. 1C-D for negative controls, 1E-F for positive controls) throughout the experiments.

Thus, to achieve a more biologically significant measure of the experimental effect, we conducted plate-based MFI data normalization and transformation and computed the z-scores of all the samples (see Methods).[19] The normalized sample values are shown in Supplementary Figure 1. An overview of the computed z-scores of all experiments can be seen in Figure 2. The means of z-scores from three independent experimental replicates were computed for all tested miRNA molecules. Based on the results, we generated a list of top-scoring miRNAs (for both positive and negative scores) that can be selected as candidate *HLA-DR* miRNA regulators. Specifically, we defined z-score +4 and -3 as the thresholds for top up- and down-regulating miRNAs, respectively (see Methods). As a result, ten up-regulating and five down-regulating miRNAs were identified for surface HLA-DR expression regulators. These are listed in Tables 1 and 2. We applied a bootstrap sensitivity analysis to further validate our identified top results. Analysis of the results confirms the Z-scoring method as a robust predictor of the up-regulating (Fig. 3A) and down-regulating (Fig. 3B) molecules.

Verification and validation of the miRNA modulation of HLA-DR expression

To verify the regulating effects on the surface HLA-DR expression during the RNAi screening, we randomly picked five out of the top ten up-regulating miRNAs and all five of the down-regulating miRNAs. These were used to carry out an independent cell transfection assay in MelJuSo cells. The FCM result is depicted in Fig. 4. All the tested miRNA molecules confirmed similar up-regulating and down-regulating protein regulatory effects, as revealed in the screening assays. These further verified the FCM-based HTP RNAi screening method.

Next, we aimed to validate the miRNA regulating effects of all the up-regulating and down-regulating hits on the *HLA-DR*A transcript level.[25] For this we collected the transfected MelJuSo cells 48 hours post transfection and performed a real-time quantitative PCR (*qPCR*) analysis. Fig. 5 shows the *HLA-DRA* mRNA expression after the miRNA transfection. Interestingly, the up-regulating effects of the miRNA hits on the mRNA level were generally not as pronounced, compared to the protein expression. On the other hand, the down-regulating effects of the miRNA hits on the mRNA level better reflected the protein expression regulation, although the treatment

with hsa-miR-1202 led to elevated *HLA-DRA* mRNA expression 48 hours post transfection, followed by decreased surface HLA-DR expression 72 hours post transfection.

Finally, we also examined the potential miRNA-regulating effects of all the up-regulating and down-regulating hits on both *HLA-DR*B*1* and *CIITA* transcript levels. Surprisingly, despite sharing comparable gene-regulating effects of both negative and positive RNAi controls on the *HLA-DRA* mRNA expression, no down-regulating effect on *HLA-DRB1* mRNA expression was detected among the five miRNA hits. On the other hand, the up-regulating effects seemed to remain to a certain degree such as they were seen with hsa-miR-214-3p, hsa-miR-4487, and hsa-miR-5003-3p (Supplementary Fig. S2). As for the *CIITA*, general up and down mRNA regulations were not obvious; however, individual up-regulating trends of a few miRNA molecules on *CIITA* expression could be observed (e.g., hsa-miR-214-3p, hsa-miR-3115, hsa-miR-4487, and hsa-miR-5003-3p), similar to the effects seen in both *HLA-DRA* and *HLA-DRB1* gene regulations (Supplementary Fig. S3). Taken together, the down-regulating effects specifically seen on *HLA-DRA* may suggest a direct interaction between the miRNAs and the *HLA-DRA* mRNA. On the other hand, those miRNAs that show similar up-regulating effects on all *HLA-DRA*, *HLA-DRB1*, and *CIITA* may have shared or overlapping underlying indirect gene regulation pathways.

Discussion

In this study, we performed flow cytometry-based high-throughput miRNA screening with the aim of identifying miRNAs with either up- or down-regulating effect on surface HLA-DR expression. By the end of the RNAi assay, we had successfully identified and validated 15 miRNA candidates that modulated *HLA-DRA* and/or surface HLA-DR expression in an APC-like human melanoma cell line, MelJuSo. In a previous study, large-scale genome-wide screening conducted by Paul and colleagues using several siRNA oligos to target each gene suggested that there are underlying genetic pathways for MHC-II antigen-presentation regulation.[16] Compared to siRNA, which is an exogenous double-strand RNA taken up by cells and targeting one specific gene, miRNA is a single-strand endogenous non-coding RNA that often targets multiple related genes belonging to the same cellular pathway or process, making it an excellent candidate as a drug target or diagnostic and biomarker tool, in addition to a therapeutic agent.[26] The RNAi process is mediated by a ribonucleoprotein called RNA-induced silencing complex (RISC). The miRNA-RISC complex recognizes and degrades, cleaves or represses the complementary mRNA, resulting in one of the key translational gene-silencing processes.[27-29] Besides post-transcriptional regulation, miRNAs can also be involved in transcriptional gene silencing.[30] Moreover, an miRNA can interact with various target mRNAs, and conversely, an mRNA can be regulated by several miRNAs.[31] Finally, empirical evidence shows that miRNAs not only can induce gene silencing but may also enhance translation by stabilizing their target mRNAs.[32]

According to our *qPCR* validation results, all but one (hsa-miR-1202) of the surface HLA-DR down-regulating miRNAs also showed a down-regulating effect on *HLA-DRA* mRNA expression. One plausible explanation is that hsa-miR-1202 may suppress HLA-DR expression via the translational (i.e., post-transcriptional) gene silencing process, while the other down-regulators may modulate *HLA-DRA* expression through transcriptional gene silencing, or more likely, through GW182-mediated mRNA degradation[29] or other indirect molecular pathways. As for the up-regulating molecules, among those which show an up-regulating effect on both HLA-DR surface protein and *HLA-DRA* (and *HLA-DRB1*) mRNA levels, indirect transcriptional regulation may be involved (e.g., hsa-miR-205-3p, hsa-miR-214-3p, hsa-miR-3115, hsa-miR-4487, and hsa-miR-5003-3p). On the other hand, for those surface HLA-DR up-regulators that did not show a clear regulating effect on the mRNA level, the regulation could be

achieved by altering the transport and/or cellular localization of HLA-DR molecules[16], or the modulation may be performed by stabilizing the mRNA and thus enhancing HLA-DR translation (e.g., hsa-miR-5581-5p, hsa-miR-5693, and hsa-miR-let-7f-2-3p).

To further validate the potential miRNA/mRNA target interactions, we adopted in silico approaches by using both the miRDB and TargetScan databases for target prediction of our candidate miRNA modulators. These database engines apply algorithms that are based on general information about interactions between the two RNA oligo sequences (e.g., seed sites and conservation).[33-35] The search results, defined by an individual score, have predicted interaction of the miRNAs hsa-miR-567, hsa-miR-1202 and hsa-miR-3972 with *HLA-DRA* mRNA at a higher level of confidence in both databases (Supplementary Tables S1 and S2). However, one should note that up to now the level of verified physiological relevance of such predicted interactions is rather minor.[36] Nevertheless, by incorporating new gene sequencing technologies and taking advantage of the increasing empirical data available, improvements in predictive power are likely with time.[37] Future research is likely to include experimental validation of the proposed functional miRNA/mRNA target pairs that fulfill well-defined experimental criteria, such as miRNA/mRNA co-expression, interaction of miRNA with a specific binding site, and miRNA effects on target protein expression and on biological function.

Clinically, HLA-DR surface expression on circulating monocytes has been adopted as a reliable indicator of clinical infection.[11] The number of HLA-DR surface molecules per monocyte decreases after a surgery[38] and remains at a down-regulated level for 48h post operation.[39] Surgical trauma is often linked to postoperative immune dysfunction, with postoperative sepsis being an especially critical condition. Specifically, major and extended surgery leads to significantly reduced expression of HLA-DR on peripheral blood monocytes[40], which has been associated with increased mortality in various clinical studies.[41-43] The pathological mechanism responsible for the suppressed immune response–for example in post-traumatically acquired sepsis–-remains unclear. A better understanding of the molecular regulation of HLA-DR will shed some light on immunoregulatory molecules in immunocompromised patients.

In recent years, microRNAs have gained recognition in clinical applications such as disease biomarkers or therapeutic interventions.[44,45] Much effort has been devoted to identifying miRNAs for human cancer diagnosis and therapy.[46-48] In perioperative and critical care medicine, on the other hand, circulating miRNAs are emerging as a novel

and promising diagnostic approach to treating sepsis.[49-51] New evidence is needed to link the underlying MHC-II dysregulation to the associated miRNA molecules, however.[52-54]

In the quest for innate immunomodulatory miRNAs for HLA-DR regulation, a greater high-throughput level of flow cytometric screening would be helpful. While the human MelJuSo cell line has provided an excellent *in vitro* platform for conducting such a screening, owing to its stable constitutive HLA-DR expression, the translatability of the screening outcome to preclinical immunology ultimately relies on comparable experimental findings using immune cell lines and/or primary leukocytes. Hence, we have tested the selected miRNA molecules using different human monocytic cell lines, and the preliminary results indeed confirmed a similar trend of regulatory effects on HLA-DR expression (unpublished data). Nevertheless, individual miRNA candidates identified through the RNAi screening may evoke different regulatory effects in primary cells, especially in an *ex vivo* whole-blood culture system that more closely resembles physiological conditions. Thus, follow-up studies using primary cells to scrutinize specific miRNA-regulating effects on HLA-DR regulation will be indispensable.

Materials and methods

Experimental set-up

Each of the original twenty-six plates of the human miRIDIAN miRNA mimic library was split into two separate plates, denoted as “A” and “B” experiments, for the follow-up RNAi screening assays. All experiments were performed three times (i.e., A1, A2, A3 and B1, B2, B3, respectively).

Flow cytometry (FCM)-based RNAi screening and miRNA transfection verification

The human melanoma cell line MelJuSo was cultured in Iscove’s modified Dulbecco’s medium (IMDM, Sigma Aldrich, Burlington, MA, USA) substituted with 10% fetal calf serum (FCS), 200 mM glutamine (Sigma Aldrich), 100 units/ml penicillin and 10 µg/ml streptomycin (Sigma Aldrich) at 37°C in 5% CO2. The human miRIDIAN miRNA mimic library (19.0, CS-001030, Dharmacon GE Healthcare, Lafayette, Colorado, USA), containing 2048 different human miRNAs (50 nM), was used for the RNAi screening. Forty-eight miRNAs were excluded in order to reach equal sample sizes on all screening plates.

An siRNA against human class II major histocompatibility complex transactivator (*CIITA*), siRNA Hs_CIITA_2 (100nM, Qiagen) was used as the positive control for down-regulation of HLA-DR. Two miRIDIAN microRNA mimics, cel-miR-67 (50nM, Dharmacon) and cel-miR-239b (50nM, Dharmacon), with sequences based on *C. elegans* miRNAs, were used as negative controls.

Moreover, a Dy547-labeled miRNA hairpin inhibitor based on the *C. elegans* miRNA cel-miR-67 was used to monitor delivery (50nM, Dharmacon). For the FCM-based high-throughput screening, MelJuSo cells were reverse transfected using DharmaFECT transfection reagent #1 (Dharmacon), with 5000 cells per well in 96-well plates.

For the miRNA transfection verification, a forward transfection was carried out independently, with up to 15,000 cells per well in 96-well plates. Overall, the transfection experiment was performed according to the manufacturer’s instructions.

In brief, the cells were either seeded one day before (i.e., forward) or resuspended on the day of transfection (i.e., reverse). The transfection mixture containing

miRNA/siRNA (50/100nM final concentration) and 0.15% DharmaFECT1 (Dharmacon) was vortexed at 40 rpm at room temperature for 20 min prior to transfection. Afterward, treatment cells were incubated at 37°C in 5% CO_2 for 72 hours. For antibody staining before FCM, cell surface HLA-DR was labeled with a monoclonal antibody against human HLA-DR (clone L243) using the DyLight™-488nm antibody labeling kit (Thermo Fischer Scientific, 46402). For FCM experiments, the BD FACSArray™ bioanalyzer (Becton Dickinson) was used with the following settings: FSC (212), SSC (362), Dy488 (345). The acquired FCM data were analyzed with FlowJo (V7.6.5) software (FlowJo, LLC, Ashland, OR, USA). The MelJuSo single cell population was gated and the median fluorescence intensities were computed for further statistical analyses.

Quantitative real-time PCR (*qPCR*)

To validate the effect of the miRNA transfection on the transcript of *HLA-DRA*, a forward transfection of all selected miRNA molecules and the positive/negative siRNA/miRNA controls (same concentrations as described above for FCM analysis) was conducted in 48-well plates with 25,000 cells per well. After treatment, cells were incubated at 37°C in 5% CO_2 for 48 hours prior to mRNA analysis. For the *qPCR* analysis, total RNA was extracted using the High Pure RNA Isolation Kit according to the manufacturer's instructions (Roche, Rotkreuz, Switzerland). RNA quality and concentration were determined using a NanoDrop 2000 spectrophotometer (Thermo Scientific, Reinach, Switzerland). Complementary DNAs (cDNAs) were synthesized using the Transcriptor High Fidelity cDNA Synthesis Kit according to the manufacturer's instructions (Roche, Rotkreuz, Switzerland). *qPCR* was performed using the TaqMan™ Fast Advanced Master Mix (Thermo Fisher #4444556) in the LightCycler® 480 instrument (Roche, Rotkreuz, Switzerland) following the user's manual, with the TaqMan™ Gene Expression Assay (Thermo Fisher #4351370) targeting three human genes *HLA-DRA, HLA-DRB1, CIITA* and two housekeeping genes glyceraldehyde-3-phosphate dehydrogenase (*GAPDH*) and hypoxanthine phosphoribosyl-transferase 1 (*HPRT1*) (Assay IDs: Hs00219575, Hs04192464, Hs00172106, Hs02758991, and Hs02800695, respectively) according to the manufacturer's recommended protocol. In addition, an identical cDNA template prepared from human MelJuSo cells was used throughout the assays as a *qPCR* calibrator. The 10 µl qPCR reaction mix consisted of 5 µl of TaqMan® Fast Advanced

Master Mix (2X), 0.5 µL of TaqMan® Assay (20X), and cDNA template in nuclease-free water.

The PCR reaction cycle conditions used were: 50°C for 2 min, 95°C for 20 s, followed by 45 cycles of 95°C for 3 s and 60°C for 30 s. The fluorescent signals were measured at the annealing/extension step. Standard curves were generated separately for the target gene and both reference genes using serial dilutions of the cDNA template. All *qPCR* reactions were performed in duplicate in 384-well plates. Data were processed using the LightCycler® 480 system software version 1.5.0, and analyzed using the advanced relative quantification module (Roche, Rotkreuz, Switzerland).

Briefly, the relative level of each gene transcript was determined as the mean crossing point (Cp) value and the ratio of the *HLA-DRA*, *HLA-DRB1*, or *CIITA* to the reference genes *GAPDH* and *HPRT1.* Each sample was compared with the same ratio in the standard sample (i.e., the calibrator). Thus, the relative quantification is calibrator normalized with efficiency correction and the result of the data analysis is expressed as a normalized ratio.

Statistical Analysis

Quality assessment and z-scores

We performed a quality assessment of the RNAi HTS assays by computing a specific parameter–the so-called Z' factor–which is commonly used in similar cell-based RNAi HTS experiments.[18,19] Briefly, the Z' factor is a screening window coefficient which is dimensionless, with simple statistical characteristics that can be readily applied to each conducted assay. In our RNAi HTS assays, cells transfected with siRNA Hs_CIITA_2 were used as the positive control group, while negative controls were made up of different treatment groups, including untreated cells, cells treated with transfection reagent DharmaFECT, and cells transfected with cel-miR-67 or cel-miR-239b. To validate all conducted experiments for single assays we computed all the Z' factors with different negative controls and only included assays with a Z' factor value higher than 0.5 for quality assurance. 25 out of 26 plates were available for the computation of plate-based statistics, including data normalization and transformation into z-scores.

To achieve a more biologically significant measure of the experimental effect, we followed a statistical method proposed by Boutros and colleagues which is intended

for cell-based RNAi screening analysis.[19] We conducted plate-based MFI data normalization by dividing each MFI measurement by the plate-wise median MFI value. The robust z-scores were then derived via the following equation

$$z_{kj} = \frac{y_{kj} - M}{\text{MAD}},$$

where M denotes the Median of the normalized plate values and MAD corresponds to the Median Absolute Deviation of the normalized plate values. Note here that positive and negative control values are entirely omitted in the normalization procedure.

Hit identification and sensitivity analysis

We defined z-scores +4 and -3 as the thresholds for up-regulating and down-regulating miRNAs, respectively, for surface HLA-DR expression. The asymmetry in threshold definition accounts for the slightly skewed distribution of z-scores (see Supplementary Fig. 4), and the choice of threshold values balances the need for high (absolute) z-scores for possible hits as well as for achieving a sufficient sample size of possible hits.

A permutation approach was chosen for sensitivity analysis to assess the range of z-scores for 15 identified hits (see Results). For each identified hit, we replaced the normalized MFI values of randomly chosen samples with the normalized MFI values of that particular hit sample and re-computed the z-score. We repeated this procedure for all possible combinations, resulting in distribution of z-scores for each hit. Both the location and width of such a z-score distribution give an indication of the robustness of the hit identification.

Statistical modeling of the FCM and qPCR

Sample size was N=3 for FCM and N=4 for qPCR. A linear mixed-effect model with a fixed effect was used for treatment (3 levels: negative control, downward regulation, and upward regulation) and a random slope was used for each plate and each treatment, thus accounting for the data structure of the experimental design. We transformed the outcome variable (MFI in the case of the verification experiment and the normalized ratio in case of qPCR) via ordered quantile normalization to ensure a normally distributed outcome in the linear mixed-effect model.[55] Estimated marginal means (EMMs) were employed to compute the contrasts of the two treatments and

compare them with the negative control samples.[56] No p-value adjustment for multiple comparisons was used, as the p-values were exploratory rather than confirmatory in this study.

Statistical significance and software

A p-value <0.05 was considered statistically significant. All analyses were performed with R version 4.0.2.[57]

Data availability statement: The data that support the findings of this study are available from the corresponding author upon reasonable request.

Ethics approval statement: not required.

Authors' contributions

Study concept and design: FS, MY-YH, CL

Acquisition of data: MS, MH (Houseman), LZ, CL, MY-YH

Analysis and interpretation of data: FS, MY-YH, CL, AH, MH (Houseman), MS, LZ, MH (Huber)

Statistics: MH (Huber), MY-YH

Drafting the manuscript: MY-YH, MH (Houseman), MH (Huber)

Revising and approval of the final version: all authors

All authors agree to be accountable for all aspects of the work and ensure that questions related to the accuracy or integrity of any part of the work are appropriately investigated and resolved.

Acknowledgments: The authors would like to thank Jeannie Wurz for proofreading and editing the manuscript, Marcel Schiff, Lena Matthiss, Azam Jamaati, and Sibylle Rohrbach for their excellent technical support, Paul Kunath, Jaison Phour, and Christoph Mathieu for their help with different pilot experiments.

The study was supported by an institutional grant from the Department of Anaesthesiology and Pain Medicine, Inselspital, Bern University Hospital, University of Bern, Bern, Switzerland (MY-YH, Gesuch Nr. HEYF-1-21).

Conflict of interest disclosure: All authors declare that they have no financial or commercial conflicts of interest.

References (EndNote X9)

1 Neefjes, J., Jongsma, M. L., Paul, P. & Bakke, O. Towards a systems understanding of MHC class I and MHC class II antigen presentation. *Nat Rev Immunol* **11**, 823-836, doi:10.1038/nri3084 (2011).

2 Viallard, J. F. *et al.* HLA-DR expression on lymphocyte subsets as a marker of disease activity in patients with systemic lupus erythematosus. *Clin Exp Immunol* **125**, 485-491, doi:10.1046/j.1365-2249.2001.01623.x (2001).

3 Saez-Cirion, A. *et al.* HIV controllers exhibit potent CD8 T cell capacity to suppress HIV infection ex vivo and peculiar cytotoxic T lymphocyte activation phenotype. *Proc Natl Acad Sci U S A* **104**, 6776-6781, doi:10.1073/pnas.0611244104 (2007).

4 Saraiva, D. P., Jacinto, A., Borralho, P., Braga, S. & Cabral, M. G. HLA-DR in Cytotoxic T Lymphocytes Predicts Breast Cancer Patients' Response to Neoadjuvant Chemotherapy. *Front Immunol* **9**, 2605, doi:10.3389/fimmu.2018.02605 (2018).

5 Monneret, G. *et al.* Persisting low monocyte human leukocyte antigen-DR expression predicts mortality in septic shock. *Intensive Care Med* **32**, 1175-1183, doi:10.1007/s00134-006-0204-8 (2006).

6 Wakefield, C. H., Carey, P. D., Foulds, S., Monson, J. R. & Guillou, P. J. Changes in major histocompatibility complex class II expression in monocytes and T cells of patients developing infection after surgery. *Br J Surg* **80**, 205-209, doi:10.1002/bjs.1800800224 (1993).

7 Venet, F. *et al.* Decreased monocyte human leukocyte antigen-DR expression after severe burn injury: Correlation with severity and secondary septic shock. *Crit Care Med* **35**, 1910-1917, doi:10.1097/01.CCM.0000275271.77350.B6 (2007).

8 Galbraith, N., Walker, S., Galandiuk, S., Gardner, S. & Polk, H. C., Jr. The Significance and Challenges of Monocyte Impairment: For the Ill Patient and the Surgeon. *Surg Infect (Larchmt)* **17**, 303-312, doi:10.1089/sur.2015.245 (2016).

9 Venet, F. & Monneret, G. Advances in the understanding and treatment of sepsis-induced immunosuppression. *Nat Rev Nephrol* **14**, 121-137, doi:10.1038/nrneph.2017.165 (2018).

10 Drewry, A. M. *et al.* Comparison of monocyte human leukocyte antigen-DR expression and stimulated tumor necrosis factor alpha production as outcome predictors in severe sepsis: a prospective observational study. *Crit Care* **20**, 334, doi:10.1186/s13054-016-1505-0 (2016).

11 Cheadle, W. G., Hershman, M. J., Wellhausen, S. R. & Polk, H. C., Jr. HLA-DR antigen expression on peripheral blood monocytes correlates with surgical infection. *Am J Surg* **161**, 639-645, doi:10.1016/0002-9610(91)91247-g (1991).

12 Jeannet, R., Daix, T., Formento, R., Feuillard, J. & Francois, B. Severe COVID-19 is associated with deep and sustained multifaceted cellular immunosuppression. *Intensive Care Med* **46**, 1769-1771, doi:10.1007/s00134-020-06127-x (2020).

13 Spinetti, T. *et al.* Reduced Monocytic Human Leukocyte Antigen-DR Expression Indicates Immunosuppression in Critically Ill COVID-19 Patients. *Anesth Analg* **131**, 993-999, doi:10.1213/ANE.0000000000005044 (2020).

14 Kox, M. *et al.* COVID-19 patients exhibit less pronounced immune suppression compared with bacterial septic shock patients. *Crit Care* **24**, 263, doi:10.1186/s13054-020-02896-5 (2020).

15 Monneret, G., Cour, M., Viel, S., Venet, F. & Argaud, L. Coronavirus disease 2019 as a particular sepsis: a 2-week follow-up of standard immunological parameters in critically ill patients. *Intensive Care Med* **46**, 1764-1765, doi:10.1007/s00134-020-06123-1 (2020).

16 Paul, P. *et al.* A Genome-wide multidimensional RNAi screen reveals pathways controlling MHC class II antigen presentation. *Cell* **145**, 268-283, doi:10.1016/j.cell.2011.03.023 (2011).
17 Wubbolts, R. *et al.* Direct vesicular transport of MHC class II molecules from lysosomal structures to the cell surface. *Journal of Cell Biology* **135**, 611-622, doi:DOI 10.1083/jcb.135.3.611 (1996).
18 Zhang, J. H., Chung, T. D. Y. & Oldenburg, K. R. A simple statistical parameter for use in evaluation and validation of high throughput screening assays. *Journal of Biomolecular Screening* **4**, 67-73, doi:Doi 10.1177/108705719900400206 (1999).
19 Boutros, M., Bras, L. P. & Huber, W. Analysis of cell-based RNAi screens. *Genome Biology* **7**, doi:ARTN R66

10.1186/gb-2006-7-7-r66 (2006).
20 Agrawal, S. & Kandimalla, E. R. Antisense and siRNA as agonists of Toll-like receptors. *Nature Biotechnology* **22**, 1533-1537, doi:10.1038/nbt1042 (2004).
21 Reynolds, A. *et al.* Induction of the interferon response by siRNA is cell type- and duplex length-dependent. *Rna* **12**, 988-993, doi:10.1261/rna.2340906 (2006).
22 Steimle, V., Otten, L. A., Zufferey, M. & Mach, B. Complementation cloning of an MHC class II transactivator mutated in hereditary MHC class II deficiency (or bare lymphocyte syndrome). *Cell* **75**, 135-146 (1993).
23 Accolla, R. S., Ramia, E., Tedeschi, A. & Forlani, G. CIITA-Driven MHC Class II Expressing Tumor Cells as Antigen Presenting Cell Performers: Toward the Construction of an Optimal Anti-tumor Vaccine. *Frontiers in Immunology* **10**, doi:ARTN 1806

10.3389/fimmu.2019.01806 (2019).
24 Denzin, L. K., Hammond, C. & Cresswell, P. HLA-DM interactions with intermediates in HLA-DR maturation and a role for HLA-DM in stabilizing empty HLA-DR molecules. *J Exp Med* **184**, 2153-2165, doi:DOI 10.1084/jem.184.6.2153 (1996).
25 Cajander, S. C. *et al.* Expression of mRNA levels of HLA-DRA in relation to monocyte HLA-DR: a longitudinal sepsis study. *Critical Care* **19**, P45, doi:10.1186/cc14125 (2015).
26 Lam, J. K. W., Chow, M. Y. T., Zhang, Y. & Leung, S. W. S. siRNA Versus miRNA as Therapeutics for Gene Silencing. *Molecular Therapy-Nucleic Acids* **4**, doi:ARTN e252

10.1038/mtna.2015.23 (2015).
27 Filipowicz, W., Bhattacharyya, S. N. & Sonenberg, N. Mechanisms of post-transcriptional regulation by microRNAs: are the answers in sight? *Nat Rev Genet* **9**, 102-114, doi:10.1038/nrg2290 (2008).
28 Bartel, D. P. MicroRNAs: target recognition and regulatory functions. *Cell* **136**, 215-233, doi:10.1016/j.cell.2009.01.002 (2009).
29 Braun, J. E., Huntzinger, E. & Izaurralde, E. A Molecular Link between miRISCs and Deadenylases Provides New Insight into the Mechanism of Gene Silencing by MicroRNAs. *Csh Perspect Biol* **4**, doi:ARTN a012328

10.1101/cshperspect.a012328 (2012).
30 Catalanotto, C., Cogoni, C. & Zardo, G. MicroRNA in Control of Gene Expression: An Overview of Nuclear Functions. *Int J Mol Sci* **17**, doi:10.3390/ijms17101712 (2016).

31 Lewis, B. P., Shih, I. H., Jones-Rhoades, M. W., Bartel, D. P. & Burge, C. B. Prediction of mammalian microRNA targets. *Cell* **115**, 787-798, doi:10.1016/s0092-8674(03)01018-3 (2003).
32 Carroll, A. P., Tran, N., Tooney, P. A. & Cairns, M. J. Alternative mRNA fates identified in microRNA-associated transcriptome analysis. *BMC Genomics* **13**, 561, doi:10.1186/1471-2164-13-561 (2012).
33 Betel, D., Koppal, A., Agius, P., Sander, C. & Leslie, C. Comprehensive modeling of microRNA targets predicts functional non-conserved and non-canonical sites. *Genome Biol* **11**, R90, doi:10.1186/gb-2010-11-8-r90 (2010).
34 Agarwal, V., Bell, G. W., Nam, J. W. & Bartel, D. P. Predicting effective microRNA target sites in mammalian mRNAs. *Elife* **4**, doi:10.7554/eLife.05005 (2015).
35 McGeary, S. E. *et al.* The biochemical basis of microRNA targeting efficacy. *Science* **366**, 1470-+, doi:ARTN eaav1741

10.1126/science.aav1741 (2019).
36 Chen, Y. & Wang, X. miRDB: an online database for prediction of functional microRNA targets. *Nucleic Acids Res* **48**, D127-D131, doi:10.1093/nar/gkz757 (2020).
37 Liu, W. & Wang, X. Prediction of functional microRNA targets by integrative modeling of microRNA binding and target expression data. *Genome Biol* **20**, 18, doi:10.1186/s13059-019-1629-z (2019).
38 Hensler, T. *et al.* Distinct mechanisms of immunosuppression as a consequence of major surgery. *Infection and Immunity* **65**, 2283-2291, doi:Doi 10.1128/Iai.65.6.2283-2291.1997 (1997).
39 Erdoes, G. *et al.* Technical Approach Determines Inflammatory Response after Surgical and Transcatheter Aortic Valve Replacement. *Plos One* **10**, doi:ARTN e0143089

10.1371/journal.pone.0143089 (2015).
40 Menges, P. *et al.* Surgical Trauma and Postoperative Immune Dysfunction. *European Surgical Research* **48**, 180-186, doi:10.1159/000338196 (2012).
41 Satoh, A. *et al.* Human leukocyte antigen-DR expression on peripheral monocytes as a predictive marker of sepsis during acute pancreatitis. *Pancreas* **25**, 245-250, doi:Doi 10.1097/00006676-200210000-00006 (2002).
42 Haveman, J. W. *et al.* HLA-DR expression on monocytes and systemic inflammation in patients with ruptured abdominal aortic aneurysms. *Critical Care* **10**, doi:ARTN R119

10.1186/cc5017 (2006).
43 Franke, A. *et al.* Delayed recovery of human leukocyte antigen-DR expression after cardiac surgery with early non-lethal postoperative complications: only an epiphenomenon? *Interact Cardiovasc Thorac Surg* **7**, 207-211, doi:10.1510/icvts.2007.158899 (2008).
44 Diener, C., Keller, A. & Meese, E. Emerging concepts of miRNA therapeutics: from cells to clinic. *Trends Genet*, doi:10.1016/j.tig.2022.02.006 (2022).
45 Chakraborty, C., Sharma, A. R., Sharma, G. & Lee, S. S. Therapeutic advances of miRNAs: A preclinical and clinical update. *J Adv Res* **28**, 127-138, doi:10.1016/j.jare.2020.08.012 (2021).
46 Peng, Y. & Croce, C. M. The role of MicroRNAs in human cancer. *Signal Transduct Tar* **1**, doi:ARTN 15004

10.1038/sigtrans.2015.4 (2016).

47 Zuckerman, J. E. & Davis, M. E. Clinical experiences with systemically administered siRNA-based therapeutics in cancer. *Nat Rev Drug Discov* **14**, 843-856, doi:10.1038/nrd4685 (2015).
48 Chalbatani, G. M. *et al.* Small interfering RNAs (siRNAs) in cancer therapy: a nano-based approach. *Int J Nanomed* **14**, 3111-3128, doi:10.2147/Ijn.S200253 (2019).
49 Essandoh, K. & Fan, G. C. Role of extracellular and intracellular microRNAs in sepsis. *Bba-Mol Basis Dis* **1842**, 2155-2162, doi:10.1016/j.bbadis.2014.07.021 (2014).
50 Szilagyi, B., Fejes, Z., Pocsi, M., Kappelmayer, J. & Nagy, B., Jr. Role of sepsis modulated circulating microRNAs. *EJIFCC* **30**, 128-145 (2019).
51 Wang, H. *et al.* Serum microRNA signatures identified by Solexa sequencing predict sepsis patients' mortality: a prospective observational study. *Plos One* **7**, e38885, doi:10.1371/journal.pone.0038885 (2012).
52 Stickel, N. *et al.* MicroRNA-146a reduces MHC-II expression via targeting JAK/STAT signaling in dendritic cells after stem cell transplantation. *Leukemia* **31**, 2732-2741, doi:10.1038/leu.2017.137 (2017).
53 Cazalis, M. A. *et al.* Decreased HLA-DR antigen-associated invariant chain (CD74) mRNA expression predicts mortality after septic shock. *Crit Care* **17**, R287, doi:10.1186/cc13150 (2013).
54 Codolo, G. *et al.* Helicobacter pylori Dampens HLA-II Expression on Macrophages via the Up-Regulation of miRNAs Targeting CIITA. *Front Immunol* **10**, doi:ARTN 2923

10.3389/fimmu.2019.02923 (2020).
55 Peterson, R. A. & Cavanaugh, J. E. Ordered quantile normalization: a semiparametric transformation built for the cross-validation era. *J Appl Stat* **47**, 2312-2327, doi:10.1080/02664763.2019.1630372 (2020).
56 emmeans: Estimated Marginal Means, aka Least-Squares Means. R package version 1.6.0. (2021).
57 R: A language and environment for statistical computing. R Foundation for Statistical Computing, Vienna, Austria. (2020).

Tables

								z-score > 4
Plate	**Col**	**Row**	**Experiment**	**Mature Name**	**Fluorescence (MFI)**	**MFI normalized**	**z-score**	**z-score (mean)**
1	3	1	B1	hsa-miR-214-3p	18372	2.18	5.87	5.86
1	3	1	B2	hsa-miR-214-3p	13327	2.75	6.03	5.86
1	3	1	B3	hsa-miR-214-3p	16344	2.01	5.68	5.86
8	8	5	A1	hsa-miR-513a-3p	23371	2.01	4.23	4.75
8	8	5	A2	hsa-miR-513a-3p	24508	2.14	7.67	4.75
8	8	5	A3	hsa-miR-513a-3p	17988	1.51	2.35	4.75
8	9	4	B1	hsa-let-7f-2-3p	15455	1.38	2.11	4.06
8	9	4	B2	hsa-let-7f-2-3p	14449	1.40	2.06	4.06
8	9	4	B3	hsa-let-7f-2-3p	34746	3.12	8.01	4.06
10	10	1	B1	hsa-miR-205-3p	25580	2.17	4.33	4.04
10	10	1	B2	hsa-miR-205-3p	24566	1.90	4.09	4.04
10	10	1	B3	hsa-miR-205-3p	22184	1.99	3.70	4.04
13	4	1	A1	hsa-miR-3115	22079	2.23	7.20	6.78
13	4	1	A2	hsa-miR-3115	28005	2.24	7.50	6.78
13	4	1	A3	hsa-miR-3115	28072	2.42	5.65	6.78
18	4	1	A1	hsa-miR-4487	20327	1.88	4.81	4.41
18	4	1	A2	hsa-miR-4487	9862	1.88	3.94	4.41
18	4	1	A3	hsa-miR-4487	13357	1.91	4.47	4.41
21	4	4	B1	hsa-miR-4753-5p	12381	2.14	3.40	4.45
21	4	4	B2	hsa-miR-4753-5p	5039	3.39	6.18	4.45
21	4	4	B3	hsa-miR-4753-5p	10156	2.03	3.77	4.45
23	7	4	A1	hsa-miR-5003-3p	7663	2.30	5.44	5.97
23	7	4	A2	hsa-miR-5003-3p	15241	2.51	5.51	5.97
23	7	4	A3	hsa-miR-5003-3p	8355	2.38	6.95	5.97
24	4	1	B1	hsa-miR-5693	8834	2.02	4.63	4.40
24	4	1	B2	hsa-miR-5693	9197	1.61	4.25	4.40
24	4	1	B3	hsa-miR-5693	6926	1.91	4.33	4.40
24	9	3	B1	hsa-miR-5581-5p	4614	1.06	0.26	4.49
24	9	3	B2	hsa-miR-5581-5p	11273	1.97	6.80	4.49
24	9	3	B3	hsa-miR-5581-5p	8524	2.36	6.42	4.49

Table 1. Median Fluorescence Intensity (MFI) values and corresponding z-scores – both individually and the mean across 3 repeats – are shown for the miRNA considered a hit with z-scores above the threshold of 4.

								z-score < -3
Plate	**Col**	**Row**	**Experiment**	**Mature Name**	**Fluorescence (MFI)**	**MFI normalized**	**z-score**	**z-score (mean)**
5	8	1	A1	hsa-miR-567	782	0.09	-6.52	-5.163333
5	8	1	A2	hsa-miR-567	737	0.07	-4.32	-5.163333
5	8	1	A3	hsa-miR-567	968	0.12	-4.65	-5.163333
7	6	4	B1	hsa-miR-151a-5p	2076	0.33	-2.72	-3.080000
7	6	4	B2	hsa-miR-151a-5p	1920	0.22	-3.17	-3.080000
7	6	4	B3	hsa-miR-151a-5p	2414	0.24	-3.35	-3.080000
10	8	3	B1	hsa-miR-1202	2181	0.19	-3.01	-3.160000
10	8	3	B2	hsa-miR-1202	2934	0.23	-3.53	-3.160000
10	8	3	B3	hsa-miR-1202	2368	0.21	-2.94	-3.160000
17	7	3	A1	hsa-miR-151b	3420	0.31	-4.00	-3.886667
17	7	3	A2	hsa-miR-151b	1322	0.25	-2.34	-3.886667
17	7	3	A3	hsa-miR-151b	1437	0.31	-5.32	-3.886667
19	6	2	B1	hsa-miR-3972	2452	0.25	-3.69	-3.983333
19	6	2	B2	hsa-miR-3972	1555	0.23	-4.84	-3.983333
19	6	2	B3	hsa-miR-3972	775	0.21	-3.42	-3.983333

Table 2. Median Fluorescence Intensity (MFI) values and corresponding z-scores – both individually and the mean across 3 repeats – are shown for the miRNA considered a hit with z-scores below the threshold of -3.

Figure legends

Figure 1. Flow cytometry (FCM) analysis of HLA-DR surface expression in a large-scale miRNA screen. Box-and-whiskers plots are used to illustrate the median values, upper and lower quartiles as well as outliers of Median Fluorescence Intensity (MFI) of the three independent experiments (N=3) of the FCM data, grouped by plate A and B (A1-A25, B1-B25) and sample types: (A) miRNA samples, (B) positive controls, and (C) negative controls.

Figure 2. Overview of the computed sample z-scores of all three experiments. Plate-based data normalization and transformation of Median Fluorescence Intensity (MFI) measurements was performed, and the MFI data were computed into z-scores (see Methods). Robust z-scores values for each plate in all three independent experiments (A1, A2, A3 and B1, B2, B3) can been seen.

Figure 3. Sensitivity analysis of the selected top up- and down-regulating miRNA molecules. Box-and-whiskers plots illustrating the median values, upper and lower quartiles as well as outliers of z-scores of each (A) up-regulating and (B) down-regulating miRNA hits in the sensitivity analysis. The sensitivity analysis is based on a permutation approach (refer to Statistical Analysis) and examines how strongly the z-scores of each hit depends on the normalized Median Fluorescence Intensity (MFI) values of the corresponding plate.

Figure 4. Regulating effect of ten selected miRNAs on HLA-DR surface expression. Flow cytometry was conducted to estimate HLA-DR surface expression 72 hours post transfection in human cell line MelJuSo. (A) Representative dot plots gating MelJuSo population, single cells, and histogram of surface HLA-DR protein expression levels in gated MelJuSo single cells transfected with different small non-coding RNA molecules (light gray: negative control miRNA mimics, dark gray: positive control siRNA targeting CIITA, blue: down-regulating miRNA, and red: up-regulating miRNA). (B) Comparison of the Median Fluorescence Intensity (MFI) of surface HLA-DR among pooled treatments groups (gray: negative control miRNA mimics based on *C. elegans* sequences, blue: down-regulating miRNAs, and red: up-regulating miRNAs). Mean MFI values per group and associated 95% confidence intervals are shown. In order to perform group comparisons, a linear mixed-effect model with a fixed effect was used for treatment (3 levels: negative control, down- and up-regulation) and a random slope was used for each experiment and each treatment (see Methods). MFI values were

transformed using Ordered Quantile normalization to ensure a normally distributed outcome in the linear mixed-effect model. Estimated marginal means (EMMs) were employed to compute the contrasts of the two treatments and compare them with the negative control samples. No p-value adjustment for multiple comparisons was used, as the p-values were exploratory rather than confirmatory in this study. (C) Mean MFIs for verification samples. Colored dots represent individual samples from three independent experiments (N=3).

Figure 5. Regulating effect of all selected miRNAs on *HLA-DRA* mRNA expression. Real-time quantitative PCR (*qPCR*) was performed to estimate *HLA-DRA* transcript expression 48 hours post transfection in human cell line MelJuSo. Two housekeeping genes glyceraldehyde-3-phosphate dehydrogenase (*GAPDH*) and hypoxanthine phosphoribosyl-transferase 1 (*HPRT1*) were used as reference genes. The relative quantification is calibrator normalized with efficiency correction and the result of the data analysis is expressed as a normalized ratio. (A) Comparison of the normalized ratio of *HLA-DRA* among pooled treatments groups (gray: negative controls of untreated cells, cells treated with transfection reagent only, and cells treated with two miRNA mimics based on *C. elegans* sequences; blue: down-regulating miRNAs; and red: up-regulating miRNAs). Mean normalized ratios per group and associated 95% confidence intervals are shown. In order to perform group comparisons, a linear mixed-effect model with a fixed effect was used for treatment (3 levels: negative control, down- and up-regulation) and a random slope was used for each experiment and each treatment (see Methods). The normalized ratio was transformed using an Ordered Quantile normalization to ensure a normally distributed outcome in the linear mixed-effect model. Estimated marginal means (EMMs) were employed to compute the contrasts of the two treatments and compare them with the negative control samples. No p-value adjustment for multiple comparisons was used, as the p-values were exploratory rather than confirmatory in this study. (B) The normalized ratios for verification samples. Colored dots represent individual samples from four independent experiments (N=4).

Supporting Information

Figure legends

Figure S1. Normalized plate-based Median Fluorescence Intensity (MFI) data of the flow cytometry (FCM) analysis of HLA-DR surface expression in a large-scale miRNA screen. Box-and-whiskers plots are used to illustrate the median, upper and lower quartiles as well as outliers of plate-based normalized MFI values of the three independent experiments (N=3) of the FCM data, grouped by plate A and B (A1-A25, B1-B25) and sample types: (A) miRNA samples, (B) positive controls, and (C) negative controls. As expected, all samples' normalized values are centered around 1 while both positive and negative controls are randomly distributed.

Figure S2. Regulating effect of all selected miRNAs on *HLA-DRB1* mRNA expression. Real-time quantitative PCR (*qPCR*) was performed to estimate *HLA-DRB1* transcript expression 48 hours post transfection in human cell line MelJuSo. Two housekeeping genes glyceraldehyde-3-phosphate dehydrogenase (*GAPDH*) and hypoxanthine phosphoribosyl-transferase 1 (*HPRT1*) were used as reference genes. The relative quantification is calibrator normalized with efficiency correction and the result of the data analysis is expressed as a normalized ratio. (A) Comparison of the normalized ratio of *HLA-DRB1* among pooled treatments groups (gray: negative controls of untreated cells, cells treated with transfection reagent only, and cells treated with two miRNA mimics based on *C. elegans* sequences; blue: down-regulating miRNAs; and red: up-regulating miRNAs). Mean normalized ratios per group and associated 95% confidence intervals are shown. In order to perform group comparisons, a linear mixed-effect model with a fixed effect was used for treatment (3 levels: negative control, down- and up-regulation) and a random slope was used for each experiment and each treatment (see Methods). The normalized ratio was transformed using an Ordered Quantile normalization to ensure a normally distributed outcome in the linear mixed-effect model. Estimated marginal means (EMMs) were employed to compute the contrasts of the two treatments and compare them with the negative control samples. No p-value adjustment for multiple comparisons was used, as the p-values were exploratory rather than confirmatory in this study. (B) The normalized ratios for verification samples. Colored dots represent individual samples from four independent experiments (N=4).

Figure S3. Regulating effect of all selected miRNAs on *CIITA* mRNA expression. Real-time quantitative PCR (*qPCR*) was performed to estimate class II major

histocompatibility complex transactivator (*CIITA*) transcript expression 48 hours post transfection in human cell line MelJuSo. Two housekeeping genes glyceraldehyde-3-phosphate dehydrogenase (*GAPDH*) and hypoxanthine phosphoribosyl-transferase 1 (*HPRT1*) were used as reference genes. The relative quantification is calibrator normalized with efficiency correction and the result of the data analysis is expressed as a normalized ratio. (A) Comparison of the normalized ratio of *CIITA* among pooled treatments groups (gray: negative controls of untreated cells, cells treated with transfection reagent only, and cells treated with two miRNA mimics based on *C. elegans* sequences; blue: down-regulating miRNAs; and red: up-regulating miRNAs). Mean normalized ratios per group and associated 95% confidence intervals are shown. In order to perform group comparisons, a linear mixed-effect model with a fixed effect was used for treatment (3 levels: negative control, down- and up-regulation) and a random slope was used for each experiment and each treatment (see Methods). The normalized ratio was transformed using an Ordered Quantile normalization to ensure a normally distributed outcome in the linear mixed-effect model. Estimated marginal means (EMMs) were employed to compute the contrasts of the two treatments and compare them with the negative control samples. No p-value adjustment for multiple comparisons was used, as the p-values were exploratory rather than confirmatory in this study. (B) The normalized ratios for verification samples. Colored dots represent individual samples from four independent experiments (N=4).

Figure S4. Distribution of individual (A) and sample-averaged (B) z-scores. The slightly skewed distribution of z-scores toward the positive values is accounted for the asymmetry in the choice of both positive (+4) and negative (-3) threshold values.

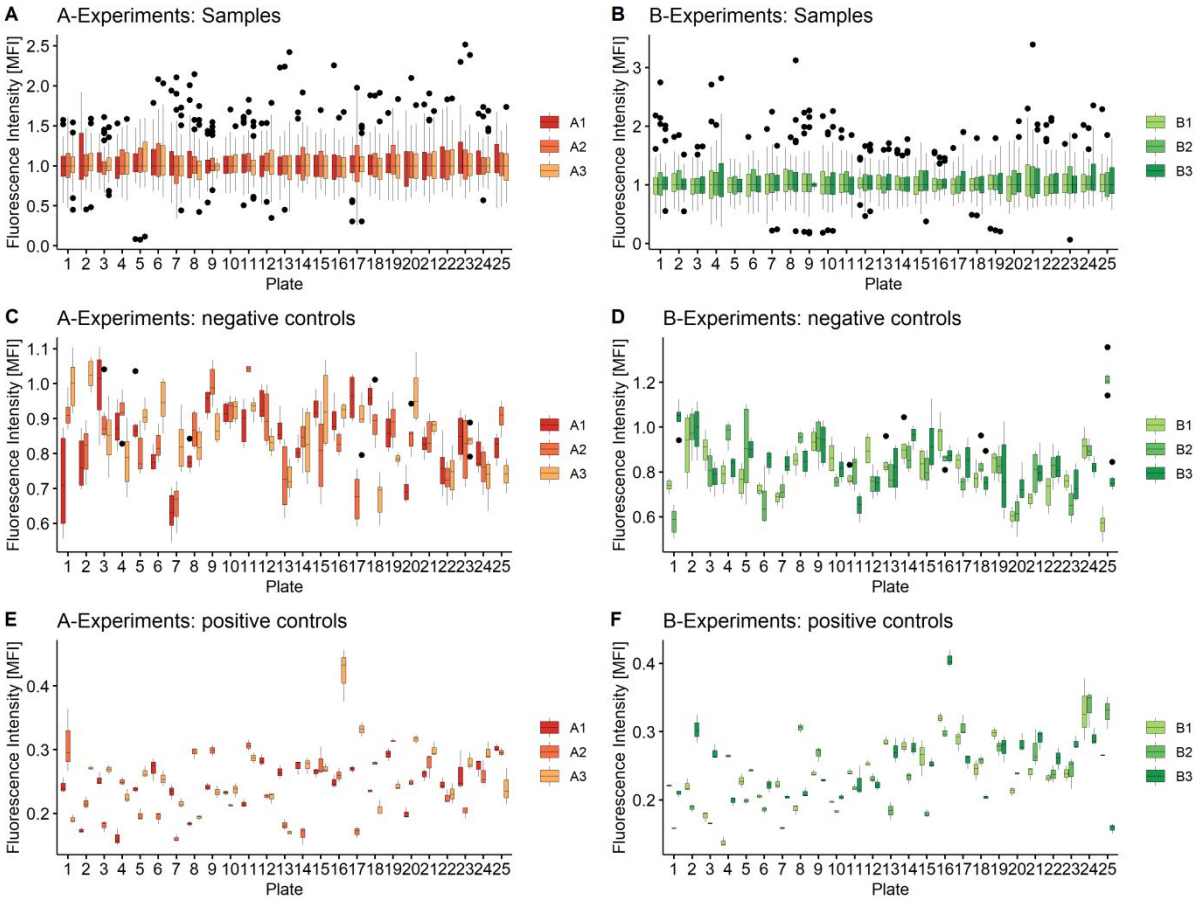

Figure S1. Normalized plate-based Median Fluorescence Intensity (MFI) data of the flow cytometry (FCM) analysis of HLA-DR surface expression in a large-scale miRNA screen. Box-and-whiskers plots are used to illustrate the median, upper and lower quartiles as well as outliers of plate-based normalized MFI values of the three independent experiments (N=3) of the FCM data, grouped by plate A and B (A1-A25, B1-B25) and sample types: (A) miRNA samples, (B) positive controls, and (C) negative controls. As expected, all samples' normalized values are centered around 1 while both positive and negative controls are randomly distributed.

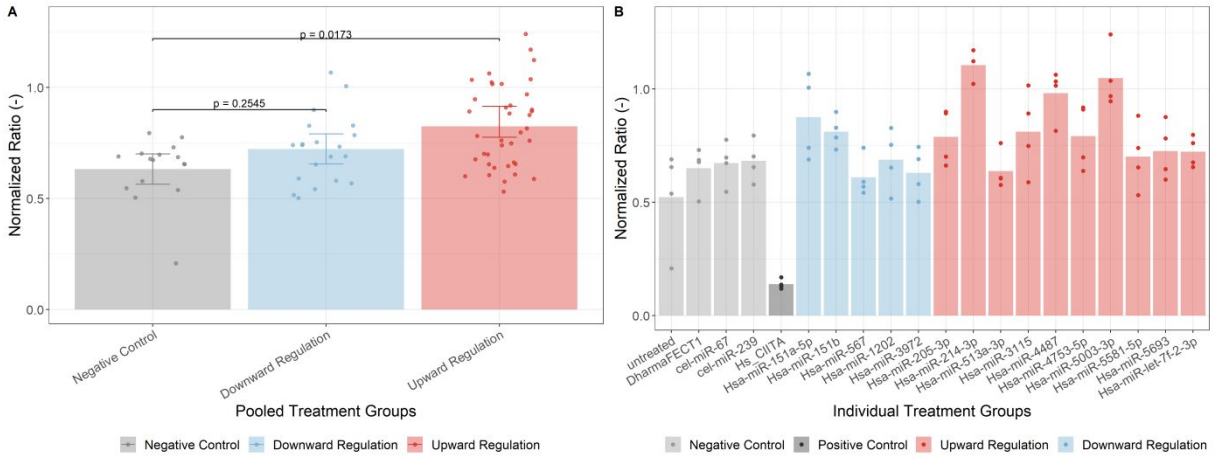

Figure S2. Regulating effect of all selected miRNAs on *HLA-DRB1* mRNA expression. Real-time quantitative PCR (*qPCR*) was performed to estimate *HLA-DRB1* transcript expression 48 hours post transfection in human cell line MelJuSo. Two housekeeping genes glyceraldehyde-3-phosphate dehydrogenase (*GAPDH*) and hypoxanthine phosphoribosyl-transferase 1 (*HPRT1*) were used as reference genes. The relative quantification is calibrator normalized with efficiency correction and the result of the data analysis is expressed as a normalized ratio. (A) Comparison of the normalized ratio of *HLA-DRB1* among pooled treatments groups (gray: negative controls of untreated cells, cells treated with transfection reagent only, and cells treated with two miRNA mimics based on *C. elegans* sequences; blue: down-regulating miRNAs; and red: up-regulating miRNAs). Mean normalized ratios per group and associated 95% confidence intervals are shown. In order to perform group comparisons, a linear mixed-effect model with a fixed effect was used for treatment (3 levels: negative control, down- and up-regulation) and a random slope was used for each experiment and each treatment (see Methods). The normalized ratio was transformed using an Ordered Quantile normalization to ensure a normally distributed outcome in the linear mixed-effect model. Estimated marginal means (EMMs) were employed to compute the contrasts of the two treatments and compare them with the negative control samples. No p-value adjustment for multiple comparisons was used, as the p-values were exploratory rather than confirmatory in this study. (B) The normalized ratios for verification samples. Colored dots represent individual samples from four independent experiments (N=4).

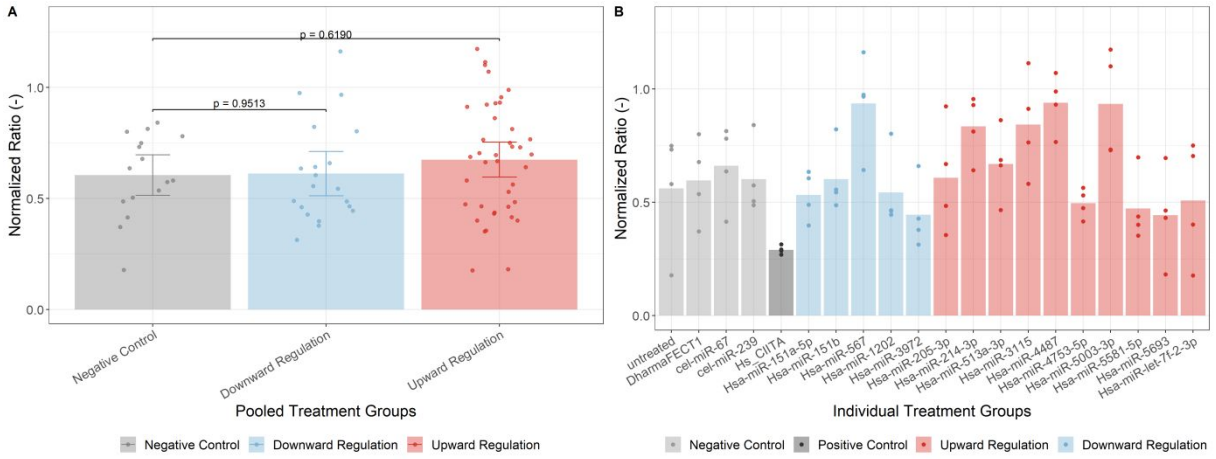

Figure S3. Regulating effect of all selected miRNAs on *CIITA* mRNA expression. Real-time quantitative PCR (*qPCR*) was performed to estimate class II major histocompatibility complex transactivator (*CIITA*) *transcript* expression 48 hours post transfection in human cell line MelJuSo. Two housekeeping genes glyceraldehyde-3-phosphate dehydrogenase (*GAPDH*) and hypoxanthine phosphoribosyl-transferase 1 (*HPRT1*) were used as reference genes. The relative quantification is calibrator normalized with efficiency correction and the result of the data analysis is expressed as a normalized ratio. (A) Comparison of the normalized ratio of *CIITA* among pooled treatments groups (gray: negative controls of untreated cells, cells treated with transfection reagent only, and cells treated with two miRNA mimics based on *C. elegans* sequences; blue: down-regulating miRNAs; and red: up-regulating miRNAs). Mean normalized ratios per group and associated 95% confidence intervals are shown. In order to perform group comparisons, a linear mixed-effect model with a fixed effect was used for treatment (3 levels: negative control, down- and up-regulation) and a random slope was used for each experiment and each treatment (see Methods). The normalized ratio was transformed using an Ordered Quantile normalization to ensure a normally distributed outcome in the linear mixed-effect model. Estimated marginal means (EMMs) were employed to compute the contrasts of the two treatments and compare them with the negative control samples. No p-value adjustment for multiple comparisons was used, as the p-values were exploratory rather than confirmatory in this study. (B) The normalized ratios for verification samples. Colored dots represent individual samples from four independent experiments (N=4).

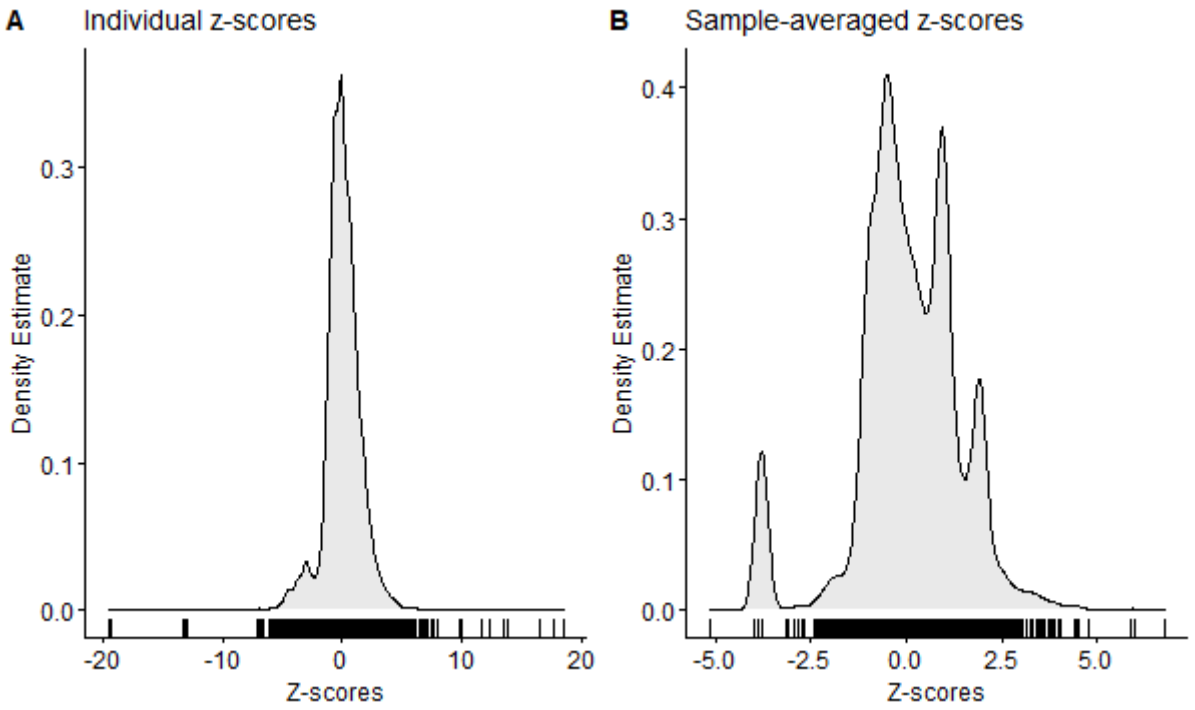

Figure S4. Distribution of individual (A) and sample-averaged (B) z-scores. The slightly skewed distribution of z-scores toward the positive values is accounted for the asymmetry in the choice of both positive (+4) and negative (-3) threshold values.

miRDB			
	HLA-DRA *NCBI Gene ID*: 3122 *Ensembl-Gene ID*: ENSG00000204287	**HLA-DRB1** *NCBI Gene ID*: 3123 *Ensembl-Gene ID*: ENSG00000196126	**CIITA** *NCBI Gene ID*: 4261 *Ensembl-Gene ID*: ENSG00000179583
miRNA			
567	81		
1202	91		
3115			
3972	91		
4487			
5693			
151a-5p			
151b			
205-3p			
214-3p			
4753-5p			
5003-3p			
513a-3p			
5581-5p			
let-7f-2-3p			

Table S1. In silico search results of target miRNA::mRNA binding prediction from the miRDB database.[36,37] Search results are shown in target scores (maximum 100), no threshold was applied.

TargetScan 8.0			
	HLA-DRA *NCBI Gene ID*: 3122 *Ensembl-Gene ID*: ENSG00000204287	**HLA-DRB1** *NCBI Gene ID*: 3123 *Ensembl-Gene ID*: ENSG00000196126	**CIITA** *NCBI Gene ID*: 4261 *Ensembl-Gene ID*: ENSG00000179583
miRNA			
567	-0,46		-0,01
1202	-0,74		
3115			
3972	-0,74		
4487			-0,12
5693			-0,13
151a-5p			
151b			
205-3p			-0,02
214-3p			-0,06
4753-5p			-0,02
5003-3p		-0,14	
513a-3p			-0,01
5581-5p			
let-7f-2-3p			-0,01

Table S2. In silico search results of target miRNA::mRNA binding prediction from the TargetScan database version 8.0. Search results are shown in cumulative weighed context scores. No threshold was applied for this depiction.

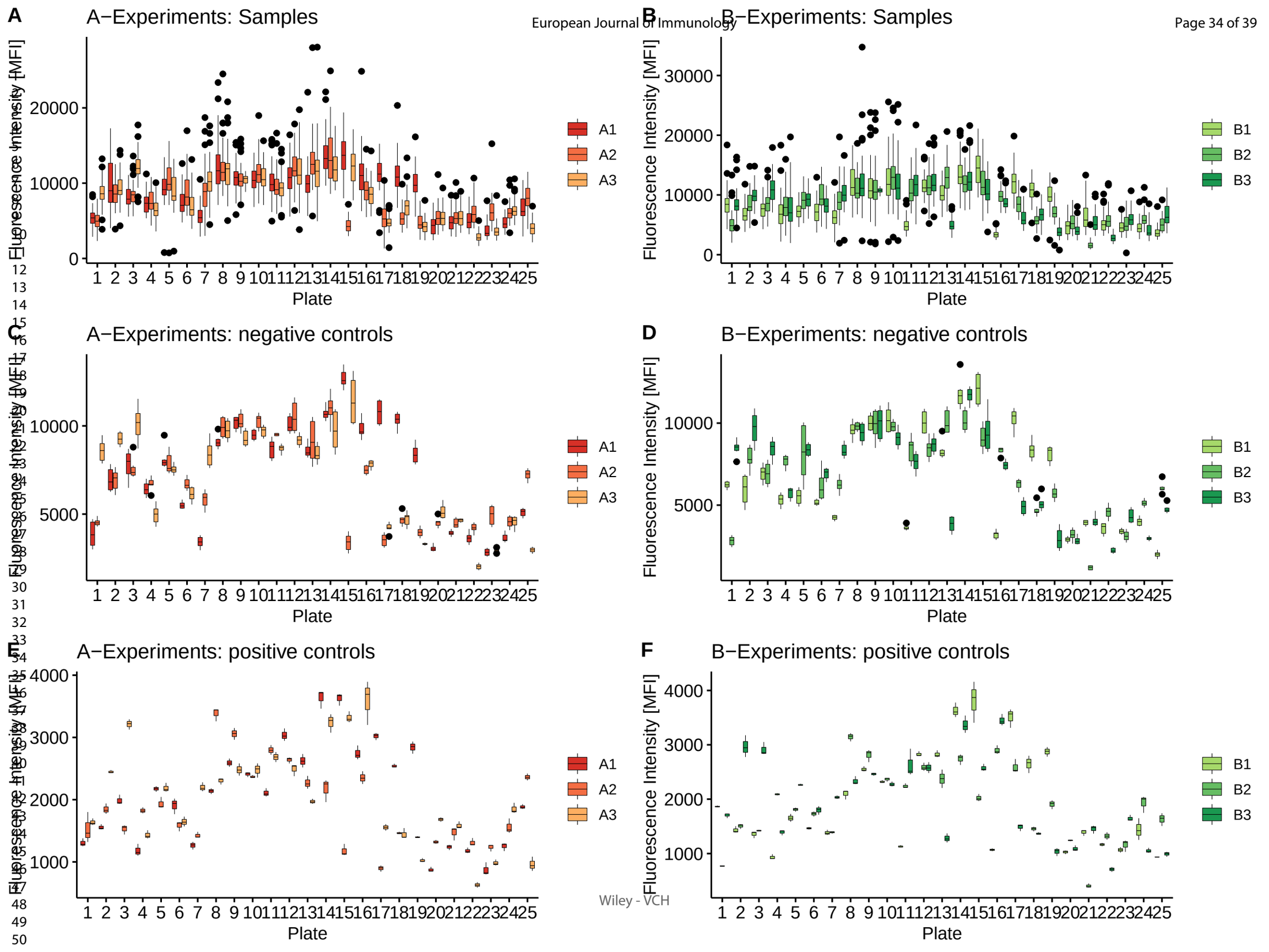
A
A−Experiments: Samples
Fluorescence Intensity [MFI]
Plate
A1
A2
A3
B
B−Experiments: Samples
Fluorescence Intensity [MFI]
Plate
B1
B2
B3
C
A−Experiments: negative controls
Fluorescence Intensity [MFI]
Plate
A1
A2
A3
D
B−Experiments: negative controls
Fluorescence Intensity [MFI]
Plate
B1
B2
B3
E
A−Experiments: positive controls
Fluorescence Intensity [MFI]
Plate
A1
A2
A3
F
B−Experiments: positive controls
Fluorescence Intensity [MFI]
Plate
B1
B2
B3

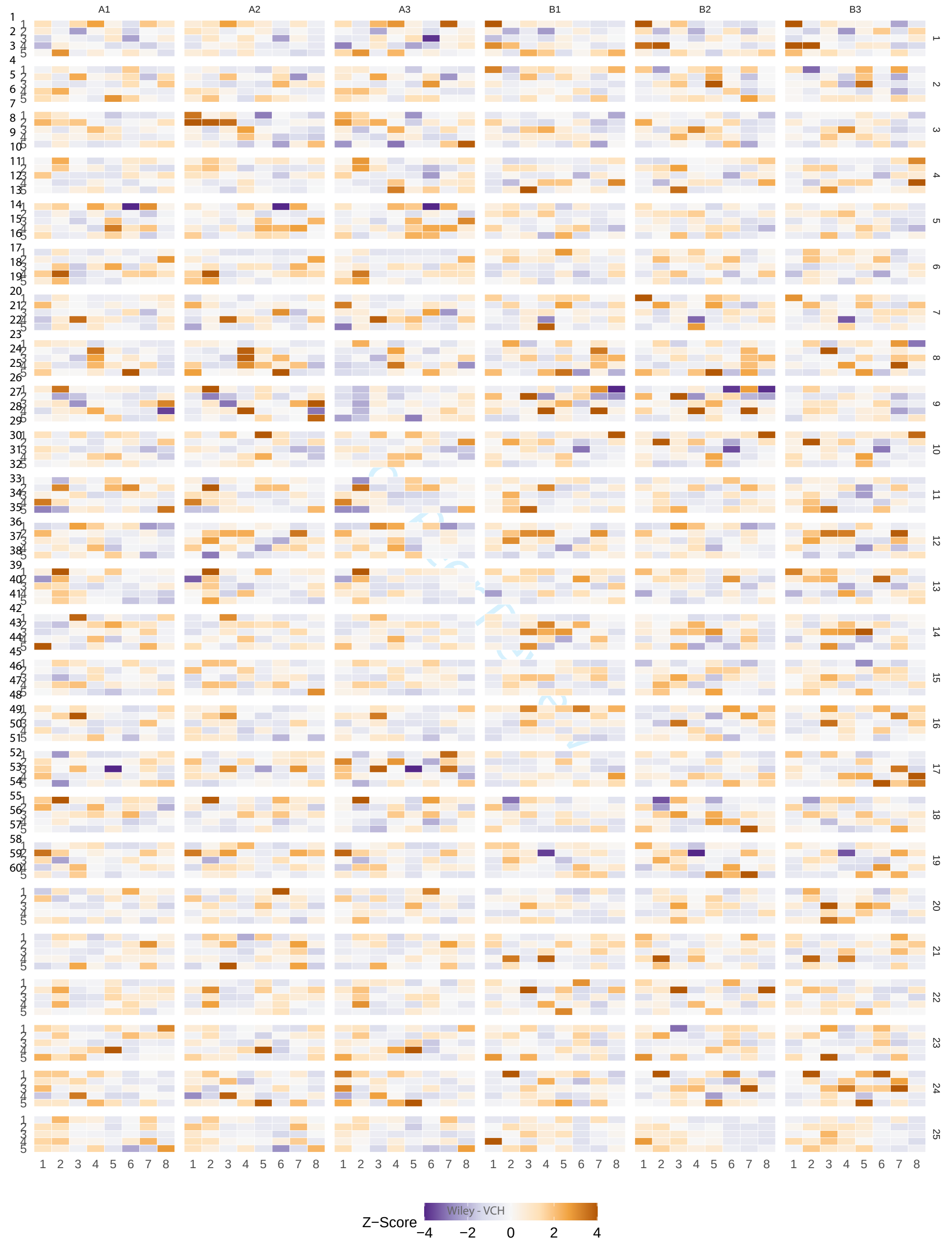
A1
A2
A3
B1
B2
B3
1 2 3 4 5 6 7 8
Z−Score
−4 −2 0 2 4
Wiley - VCH

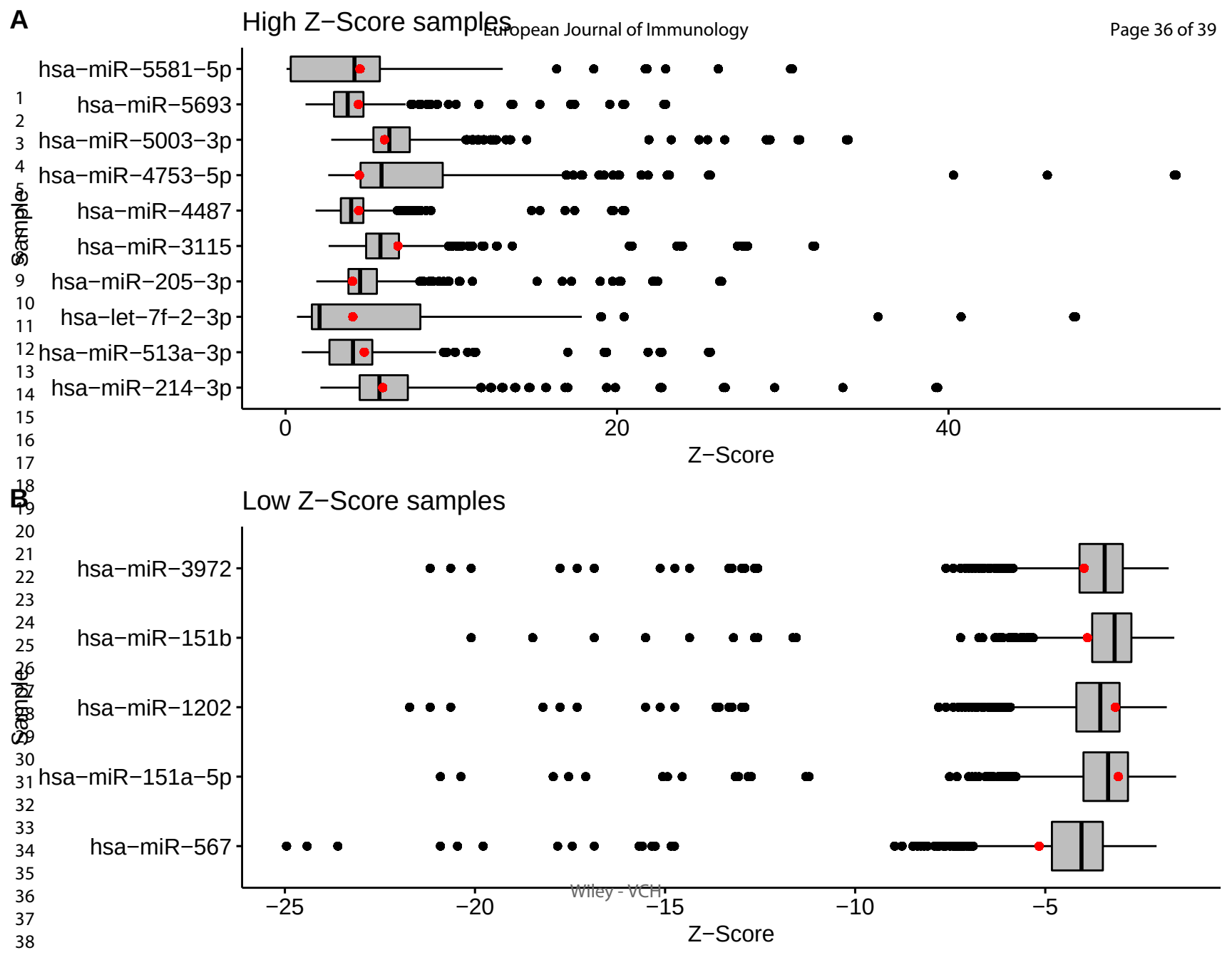
A
High Z−Score samples
hsa−miR−5581−5p
hsa−miR−5693
hsa−miR−5003−3p
hsa−miR−4753−5p
hsa−miR−4487
hsa−miR−3115
hsa−miR−205−3p
hsa−let−7f−2−3p
hsa−miR−513a−3p
hsa−miR−214−3p
Sample
0
20
40
Z−Score
B
Low Z−Score samples
hsa−miR−3972
hsa−miR−151b
hsa−miR−1202
hsa−miR−151a−5p
hsa−miR−567
Sample
−25
−20
−15
−10
−5
Z−Score

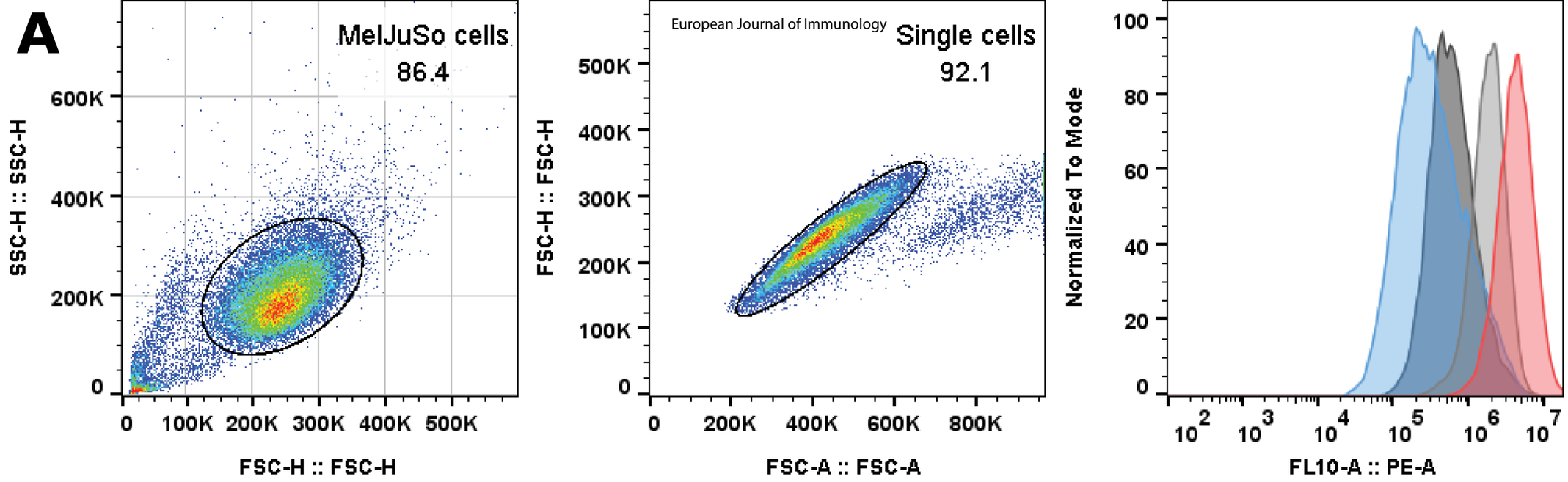
A
MelJuSo cells
86.4
SSC-H :: SSC-H
FSC-H :: FSC-H
Single cells
92.1
FSC-H :: FSC-H
FSC-A :: FSC-A
Normalized To Mode
FL10-A :: PE-A

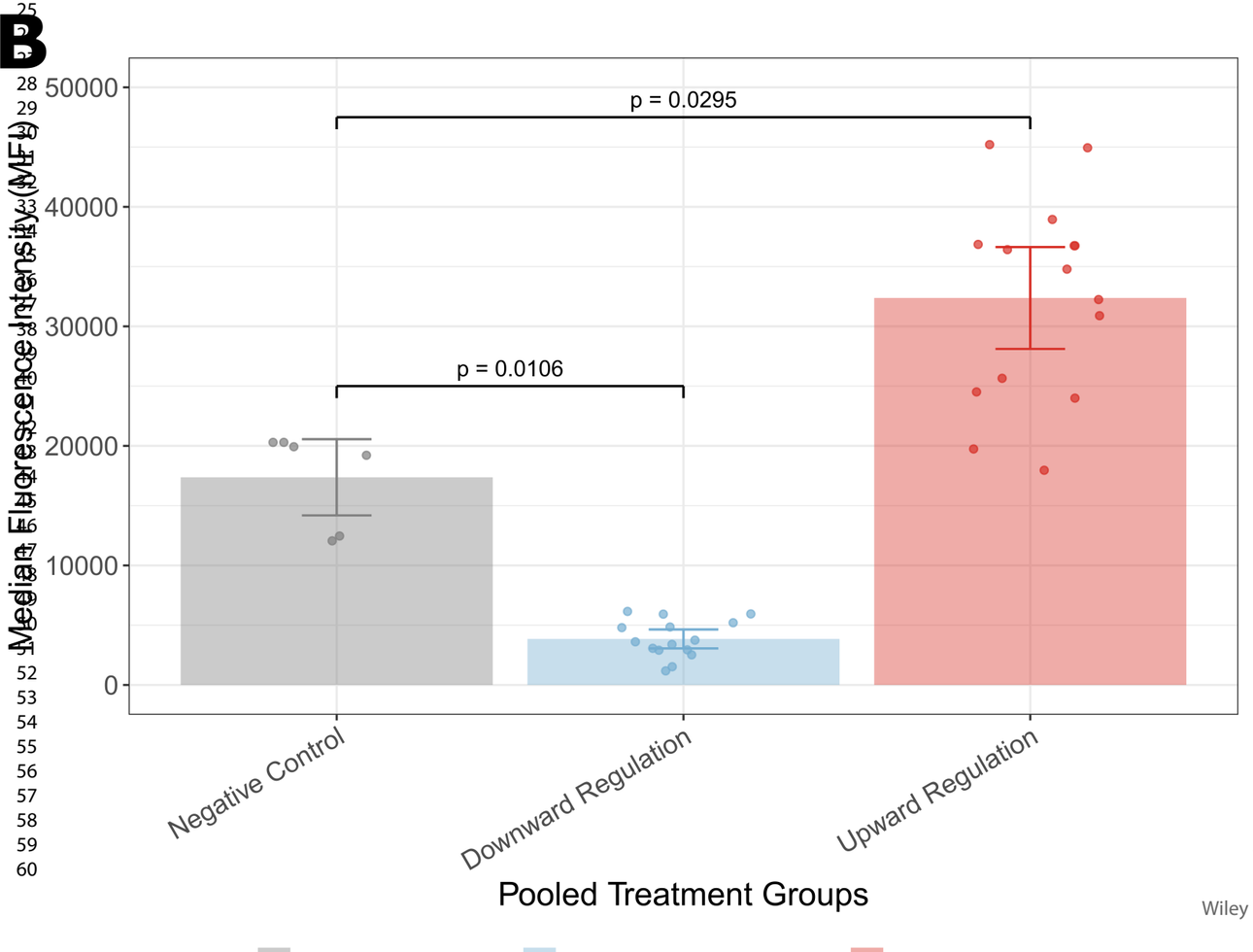
B
p = 0.0295
p = 0.0106
Median Fluorescence Intensity (MFI)
Negative Control
Downward Regulation
Upward Regulation
Pooled Treatment Groups

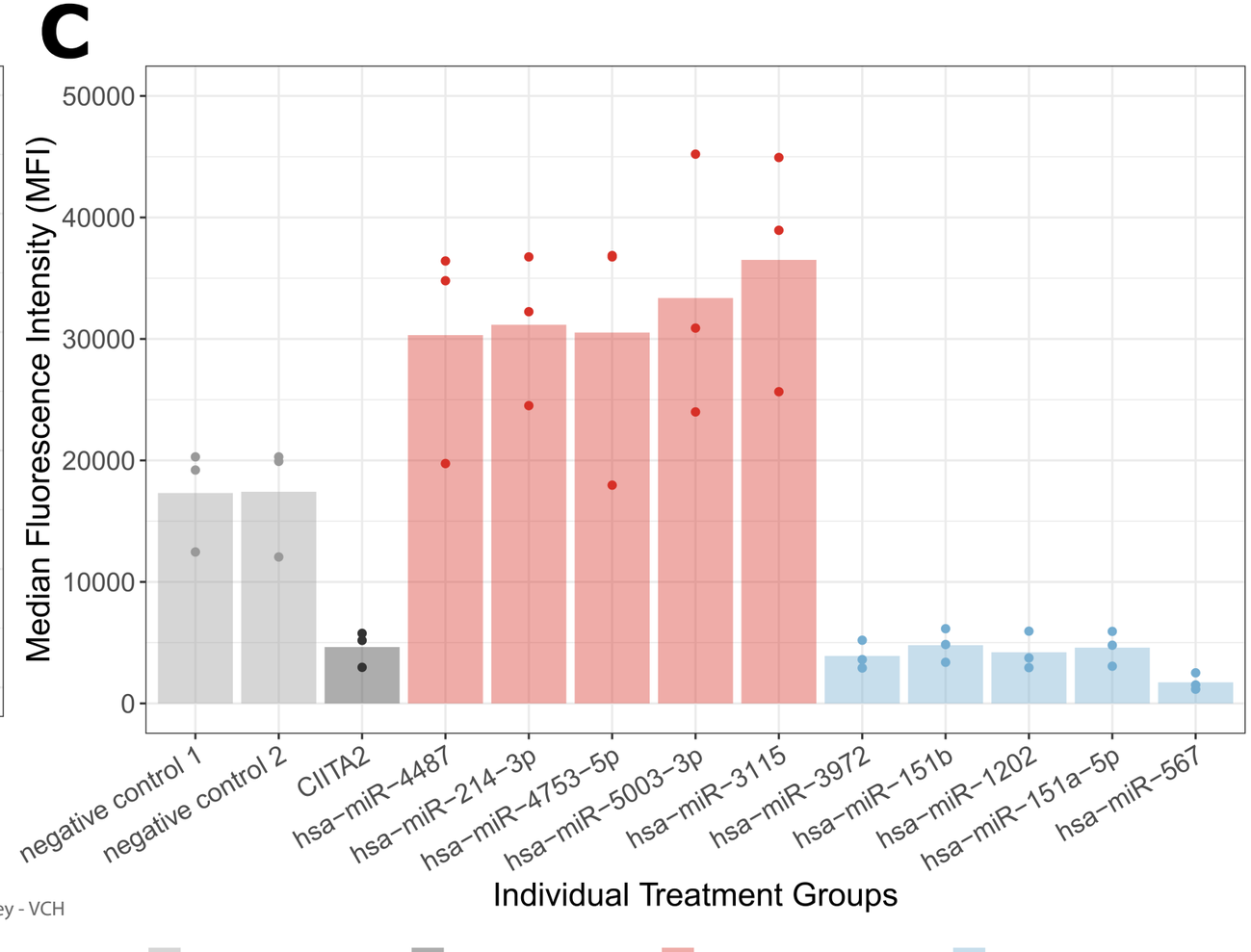
C
Median Fluorescence Intensity (MFI)
negative control 1
negative control 2
CIITA2
hsa−miR−4487
hsa−miR−214−3p
hsa−miR−4753−5p
hsa−miR−5003−3p
hsa−miR−3115
hsa−miR−3972
hsa−miR−151b
hsa−miR−1202
hsa−miR−151a−5p
hsa−miR−567
Individual Treatment Groups
Negative Control
Positive Control
Upward Regulation
Downward Regulation

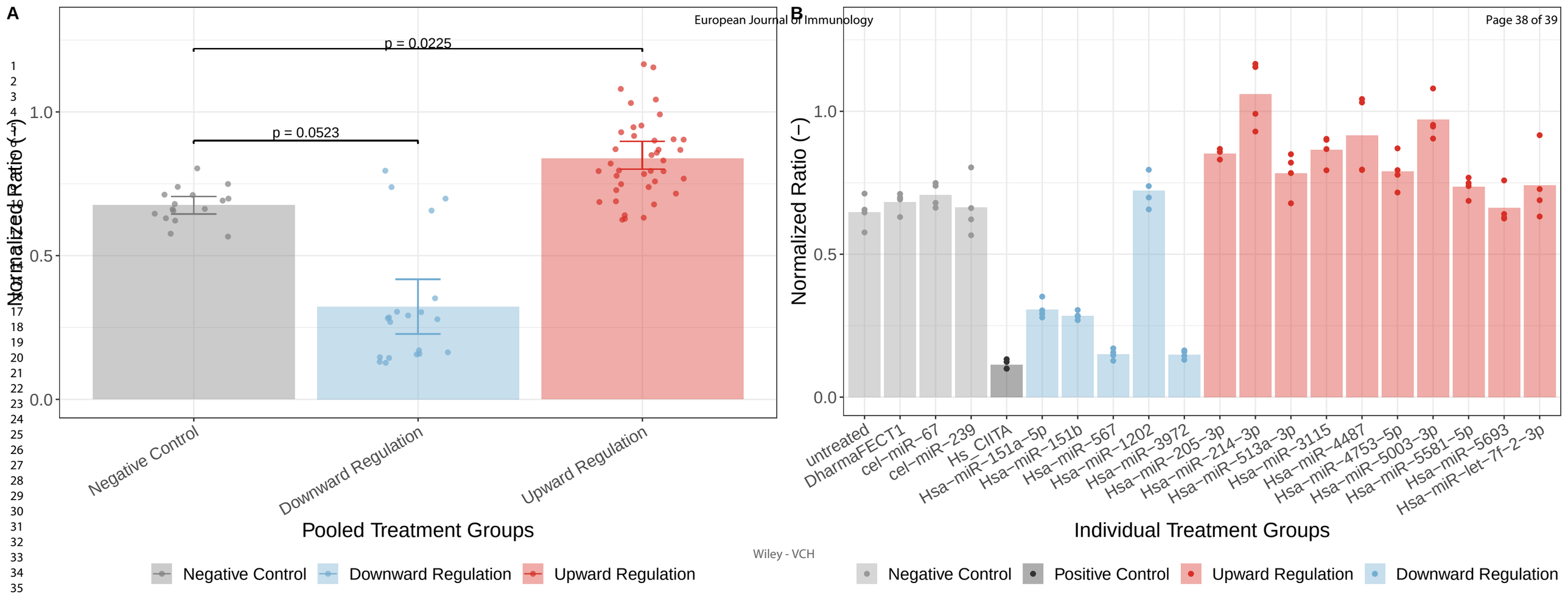
A
p = 0.0225
p = 0.0523
Normalized Ratio (−)
1.0
0.5
0.0
Negative Control
Downward Regulation
Upward Regulation
Pooled Treatment Groups
B
Normalized Ratio (−)
1.0
0.5
0.0
untreated
DharmaFECT1
cel−miR−67
cel−miR−239
Hs_CIITA
Hsa−miR−151a−5p
Hsa−miR−151b
Hsa−miR−567
Hsa−miR−1202
Hsa−miR−3972
Hsa−miR−205−3p
Hsa−miR−214−3p
Hsa−miR−513a−3p
Hsa−miR−3115
Hsa−miR−4487
Hsa−miR−4753−5p
Hsa−miR−5003−3p
Hsa−miR−5581−5p
Hsa−miR−5693
Hsa−miR−let−7f−2−3p
Individual Treatment Groups
Negative Control
Downward Regulation
Upward Regulation
Negative Control
Positive Control
Upward Regulation
Downward Regulation

Flow cytometry-based high-throughput RNAi screening has identified ten up- and five down-regulating microRNAs of the surface HLA-DR expression. The study has brought more insight to the miRNA-mediated HLA-DR regulation under both physiological and pathological conditions and may pave the way for potential clinical applications.